Dual Roles of Group IID Phospholipase A$_2$ in Inflammation and Cancer[*]

Yoshimi Miki[‡], Yuh Kidoguchi[‡§], Mariko Sato[‡§], Yoshitaka Taketomi[‡], Choji Taya[¶], Kazuaki Muramatsu[§], Michael H. Gelb[‖], Kei Yamamoto[‡**‡‡], and Makoto Murakami[‡§§1]

From the [‡]Lipid Metabolism Project and [¶]Center for Basic Technology Research, Tokyo Metropolitan Institute of Medical Science, Tokyo 156-8506, Japan, the [§]School of Science and Engineering, Tokyo Denki University, Saitama 350-0394, Japan, the [‖]Departments of Chemistry and Biochemistry, University of Washington, Seattle, Washington 98195, the [**]Faculty of Bioscience and Bioindustry, Tokushima University, Tokushima 770-8513, Japan, and [‡‡]PRIME and [§§]AMED-CREST, Japan Agency for Medical Research and Development, Tokyo 100-0004, Japan

Phospholipase A$_2$ enzymes have long been implicated in the promotion of inflammation by mobilizing pro-inflammatory lipid mediators, yet recent evidence suggests that they also contribute to anti-inflammatory or pro-resolving programs. Group IID-secreted phospholipase A$_2$ (sPLA$_2$-IID) is abundantly expressed in dendritic cells in lymphoid tissues and resolves the Th1 immune response by controlling the steady-state levels of anti-inflammatory lipids such as docosahexaenoic acid and its metabolites. Here, we show that psoriasis and contact dermatitis were exacerbated in *Pla2g2d*-null mice, whereas they were ameliorated in *Pla2g2d*-overexpressing transgenic mice, relative to littermate wild-type mice. These phenotypes were associated with concomitant alterations in the tissue levels of ω3 polyunsaturated fatty acid (PUFA) metabolites, which had the capacity to reduce the expression of pro-inflammatory and Th1/Th17-type cytokines in dendritic cells or lymph node cells. In the context of cancer, however, *Pla2g2d* deficiency resulted in marked attenuation of skin carcinogenesis, likely because of the augmented anti-tumor immunity. Altogether, these results underscore a general role of sPLA$_2$-IID as an immunosuppressive sPLA$_2$ that allows the microenvironmental lipid balance toward an anti-inflammatory state, exerting beneficial or detrimental impact depending upon distinct pathophysiological contexts in inflammation and cancer.

Endogenous mechanisms that orchestrate the resolution of inflammation are essential for tissue homeostasis. When the resolution pathways are defective, acute inflammation can progress to chronic inflammation linked to fibrosis, metabolic diseases, and cancer (1–3). Lipid mediators derived from arachidonic acid (AA),[2] including prostaglandins (PGs) and leukotrienes, are well known for their promoting roles in various inflammatory diseases, although they can also suppress immune responses under certain conditions (4, 5). Resolution of inflammation is also governed by specialized anti-inflammatory or pro-resolving lipid mediators, such as ω6 AA-derived lipoxins and ω3 polyunsaturated fatty acid (PUFA)-derived resolvins, protectins, and maresins (6, 7). Uncontrolled anti-inflammatory lipid programs perturb migration, clearance, polarization, and functions of neutrophils, macrophages, dendritic cells (DCs), and lymphocytes, leading to exacerbation of acute and chronic inflammation (8–14).

Phospholipase A$_2$ (PLA$_2$) is a group of lipolytic enzymes that hydrolyze the *sn*-2 position of glycerophospholipids to yield fatty acids and lysophospholipids. It has been established that group IVA cytosolic PLA$_2$ (cPLA$_2\alpha$) plays a central role in releasing ω6 AA toward eicosanoid generation (15–17). The secreted PLA$_2$ (sPLA$_2$) family comprises the largest PLA$_2$ subgroup with 10 catalytically active isoforms, each of which displays distinct tissue distribution and substrate selectivity (18–20). Although sPLA$_2$s have been implicated in inflammation over the last few decades, their precise biological roles have remained enigmatic until recently. Recent studies using gene-manipulated mice for sPLA$_2$s have revealed that they display pro- or anti-inflammatory functions or even inflammation-unrelated functions by driving unique lipid pathways in response to specific extracellular microenvironmental cues (12, 14, 21–27). The mobilization of distinct lipids by sPLA$_2$s appears to rely not only on their intrinsic enzymatic properties, but also tissue- or disease-specific contexts such as the lipid composition of target membranes or the spatial and temporal availability of downstream lipid-editing enzymes (18), which may account for why sPLA$_2$s exert pro- or anti-inflammatory functions with different lipid mediator profiles in distinct settings.

Group IID sPLA$_2$ (sPLA$_2$-IID) is preferentially and abundantly expressed in DCs in lymphoid organs (12), suggesting its regulatory role in acquired immunity. Indeed, a recent study

using *Pla2g2d$^{-/-}$* mice have revealed that sPLA$_2$-IID alleviates a Th1-driven immune response in the elicitation phase of contact hypersensitivity (CHS) by decreasing the level of ω3 PUFAs and their metabolites such as DHA-derived resolvin D1 (RvD1) in draining lymph nodes (LNs) (12). In addition, sPLA$_2$-IID prevents an anti-virus Th1 immune response by directing the anti-inflammatory PGD$_2$-DP1 (PGD$_2$ receptor) axis, which prevents DC migration and thereby enhances viral infection and associated lung inflammation (28). Moreover, administration of sPLA$_2$-IID-Fc protein to mice attenuates experimental autoimmune encephalomyelitis and colitis (29). To extend our understanding of the biological functions of sPLA$_2$-IID, we herein investigated the roles of this particular sPLA$_2$ in several disease models, including contact dermatitis, psoriasis, and skin cancer using *Pla2g2d*-deficient (*Pla2g2d$^{-/-}$*) and *Pla2g2d*-overexpressing transgenic (*Pla2g2d*-TG) mice. Our results point to a general role of sPLA$_2$-IID as an immunosuppressive sPLA$_2$ that alters the steady-state lipid balance toward an anti-inflammatory state, thereby providing significant impacts on inflammation and cancer.

Results

Aggravated LN Inflammation in the Late Stage of Irritant Dermatitis in Pla2g2d$^{-/-}$ Mice—In a model of CHS, application of the hapten antigen dinitrofluorobenzene (DNFB) to abdominal skin (sensitization) followed by a second application of the same antigen to ear skin (elicitation) elicits Th1-driven ear swelling (13). We have recently shown that, in the elicitation phase of CHS, the resolution of a pro-inflammatory Th1 response in the skin and regional LNs is markedly delayed in *Pla2g2d$^{-/-}$* mice (12). However, the role of sPLA$_2$-IID in acute inflammation remained unclear. We therefore examined the effect of *Pla2g2d* ablation on acute inflammation in the sensitization phase of CHS, which is equivalent to irritant dermatitis, as a model system.

Consistent with the view that *Pla2g2d* expression in DCs or macrophages is down-regulated after cell activation (12, 29), its steady-state expression in the LNs was very high (day −5, in accordance with the procedure of CHS; Fig. 1*A*) and markedly decreased 5 days after DNFB application (day 0) (Fig. 1*A*, *bottom panel*). Acute dermal edema (Fig. 1*B*) and migration of antigen-captured skin DCs to the regional LNs (12), which occurred within 24 h after DNFB treatment, did not differ between *Pla2g2d$^{+/+}$* and *Pla2g2d$^{-/-}$* mice. However, we noticed that on day 0 (*i.e.* 5 days after DNFB treatment), LN expression of the inflammatory DC/macrophage markers *Itgax* (CD11c) and *Itgam* (CD11b) was significantly greater in *Pla2g2d$^{-/-}$* mice than in *Pla2g2d$^{+/+}$* mice (Fig. 1*C*). When LN cells isolated from DNFB-treated mice were cultured *ex vivo*, *Pla2g2d$^{-/-}$* cells produced more IFN-γ, a signature Th1 cytokine, than did *Pla2g2d$^{+/+}$* cells over 48 h (Fig. 1*D*). These results suggest that *Pla2g2d* deficiency results in exacerbation of the late stage of acute inflammation toward a Th1 response in skin-regional LNs, a tissue in which sPLA$_2$-IID is abundantly expressed. Although *Pla2g2d* deficiency did not profoundly affect the increased (*Ccl2* and *Ccr5*) or constitutive (*Ccl19* and *Ccr7*) expression of DC/macrophage-attracting chemokines or chemokine receptors in the LNs on day 0, the expression of

Crth2, which encodes the pro-inflammatory chemotactic PGD$_2$ receptor CRTH2/DP2 (30, 31), was robustly elevated in DNFB-treated *Pla2g2d$^{-/-}$* LNs over *Pla2g2d$^{+/+}$* LNs (Fig. 1*E*). The LN expression of *Crth2* was much higher than that of *Ptgdr* (DP1), another PGD$_2$ receptor that prevents DC migration (28, 32). In addition, the expression of *Ptgds2*, a major PGD$_2$ synthase in the LNs, was greater in *Pla2g2d$^{-/-}$* mice than in *Pla2g2d$^{+/+}$* mice (Fig. 1*E*).

Electrospray ionization mass spectrometry (ESI-MS) analysis of lipids in the regional LNs under the steady-state condition (*i.e.* on day −5) revealed that the levels of ω3 PUFAs and their oxygenated metabolites were markedly reduced in *Pla2g2d$^{-/-}$* mice relative to *Pla2g2d$^{+/+}$* mice (Fig. 1*F*). Although the level of ω6 AA was also lower in *Pla2g2d$^{-/-}$* mice than in *Pla2g2d$^{+/+}$* mice, the levels of AA metabolites (*i.e.* PGs) were barely affected by *Pla2g2d* deficiency. These lipid profiles are consistent with our previous study and imply again that sPLA$_2$-IID is preferentially coupled with the production of ω3 PUFA metabolites, whereas PGs are mainly produced from an sPLA$_2$-IID-independent AA pool, most likely through the action of cPLA$_2$α (12). After 5 days of DNFB application (day 0), however, differences in the LN levels of PUFAs between the genotypes became smaller (Fig. 1*G*), and the RvD1 level in *Pla2g2d$^{+/+}$* LNs was markedly decreased to a level similar to that in *Pla2g2d$^{-/-}$* LNs (Fig. 1*H*), being attributable, in part, to the down-regulation of *Pla2g2d* expression (Fig. 1*A*). Exceptionally, the LN level of PGD$_2$, but not PGE$_2$, was greatly increased in *Pla2g2d$^{-/-}$* mice relative to *Pla2g2d$^{+/+}$* mice on day 0 (Fig. 1*G*), corroborating the increased expression of *Ptgds2* in the null mice (Fig. 1*E*). Moreover, when LN cells from DNFB-treated mice on day 0 were stimulated with dinitrobenzene sulfonic acid (DNBS; a water-soluble form of DNFB) for 24 h *ex vivo*, PGD$_2$ production, which depends on cPLA$_2$α (15–17), was significantly greater in *Pla2g2d$^{-/-}$* cells than in *Pla2g2d$^{+/+}$* cells (Fig. 1*I*). These results suggest that the lack of sPLA$_2$-IID exacerbates the late stage of LN inflammation in the process of irritant dermatitis with augmentation of the pro-inflammatory PGD$_2$-CRTH2 axis and an immunological shift toward an increased Th1 immune response, which may be dependent on the steady-state reduction of ω3 PUFA metabolites.

Exacerbated Psoriasis in Pla2g2d$^{-/-}$ Mice—The marked decrease in the steady-state level of ω3 PUFA metabolites in *Pla2g2d$^{-/-}$* LNs suggests that sPLA$_2$-IID could also influence other types of immune response. To address this possibility, we next examined the effect of *Pla2g2d* ablation on psoriasis, a chronic inflammatory skin disease characterized by epidermal hyperplasia (acanthosis) due to aberrant proliferation and differentiation of keratinocytes, scaling, erythematous plaque formation, and increased production of pro-inflammatory (*e.g.* TNFα) and Th17-type (*e.g.* IL-17A, IL-22, and IL-23) cytokines. In a model of imiquimod (IMQ)-induced psoriasis (33), repeated IMQ challenges to mouse ears elicit psoriasis-like acanthosis and dermal swelling with Th17-type immune responses (a schema of the procedure is illustrated in Fig. 2*A*).

We found that IMQ-induced ear swelling and epidermal hyperplasia were significantly greater in *Pla2g2d$^{-/-}$* mice than in *Pla2g2d$^{+/+}$* mice (Fig. 2, *A–C*). On day 6, the sPLA$_2$-IID signal was colocalized in most, if not all, CD11c$^+$MHC-II$^+$ der-
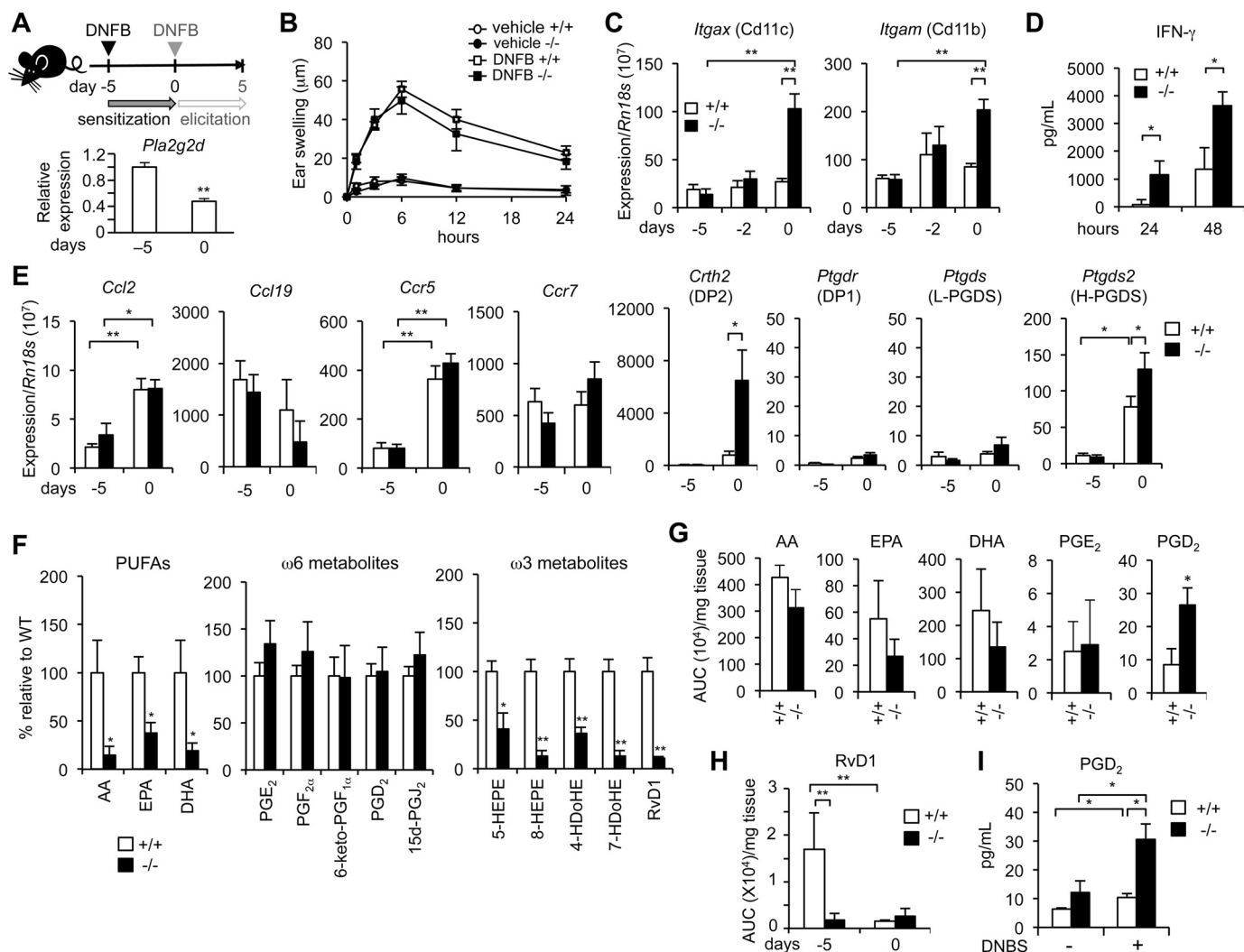
FIGURE 1. **Increased LN inflammation in the late phase of irritant dermatitis in *Pla2g2d*⁻/⁻ mice.** *A*, schematic representation of the procedure (*top panel*) and the LN expression of *Pla2g2d*, with the expression on day −5 being regarded as 1 (*n* = 4–5) (*bottom panel*), in the CHS model. The sensitization phase (irritant dermatitis) was analyzed in this study. The elicitation phase was detailed in our previous report (12). *B*, time course of ear swelling in *Pla2g2d*⁺/⁺ and *Pla2g2d*⁻/⁻ mice with or without a single application of DNFB (*n* = 6). *C*, quantitative RT-PCR of *Itgax* and *Itgam* in the draining LNs of *Pla2g2d*⁺/⁺ and *Pla2g2d*⁻/⁻ mice treated for the indicated periods with DNFB, with *Rn18s* as a normalization control (*n* = 3–4). *D*, IFN-γ production by LN cells that were obtained from DNFB-treated *Pla2g2d*⁺/⁺ and *Pla2g2d*⁻/⁻ mice on day 0 and then stimulated with DNBS for 24 or 48 h *ex vivo* (*n* = 4). *E*, quantitative RT-PCR of genes related to chemokines and lipid mediators in the LNs of *Pla2g2d*⁺/⁺ and *Pla2g2d*⁻/⁻ mice, with *Rn18s* as a normalization control (*n* = 3–6). *F*, ESI-MS analysis of the steady-state levels of PUFAs and their metabolites in the LNs of *Pla2g2d*⁺/⁺ and *Pla2g2d*⁻/⁻ mice, with the level of each lipid in *Pla2g2d*⁺/⁺ mice as 1 (*n* = 5). *G* and *H*, ESI-MS analysis of PUFAs and their metabolites in the LNs of *Pla2g2d*⁺/⁺ and *Pla2g2d*⁻/⁻ mice after treatment with DNFB for 5 days (*G*) or for the indicated periods (*H*) (*n* = 3–5). *I*, PGD₂ production by LN cells that were obtained from DNFB-treated *Pla2g2d*⁺/⁺ and *Pla2g2d*⁻/⁻ mice on day 0 and then treated with or without DNBS for 24 h *ex vivo* (*n* = 4). Values are mean ± S.E. *, *p* < 0.05, and **, *p* < 0.01.

mal DCs in the affected skin of WT mice (Fig. 2*D*). Quantitative RT-PCR of the skin and draining LNs revealed that the expression levels of Th17-related cytokines (*Il17a* and *Il22*) and chemokine (*Ccl20*) were substantially higher in IMQ-treated *Pla2g2d*⁻/⁻ mice than in *Pla2g2d*⁺/⁺ mice (Fig. 2, *E* and *F*), implying an increased Th17-type immune response in null mice. However, in contrast to sPLA₂-IIF, an epidermal sPLA₂ whose gene ablation leads to perturbed keratinocyte differentiation and activation (24), *Pla2g2d* deficiency did not affect the expression of the keratinocyte differentiation marker *Krt1* (Fig. 2*E*). Consistent with the anti-inflammatory aspect of sPLA₂-IID (see above), LN expression of *Pla2g2d* in WT mice tended to decrease following IMQ treatment (Fig. 2*F*). Flow cytometry of IL-17A- or IL-22-expressing CD3ε⁺ T cells in the skin further supported the greater Th17 response in IMQ-treated and

even IMQ-untreated *Pla2g2d*⁻/⁻ mice than in replicate *Pla2g2d*⁺/⁺ mice (Fig. 2*G*). Lipidomics analysis of the affected skin revealed substantial reductions of DHA-derived metabolites such as RvD1 (7,8,17-trihydroxy-DHA) and RvD5 (7,17-dihydroxy-DHA) but not AA-derived eicosanoids such as PGE₂ and PGD₂ in *Pla2g2d*⁻/⁻ mice relative to *Pla2g2d*⁺/⁺ mice (Fig. 2*H*). Thus, *Pla2g2d* deficiency leads to exacerbation of the Th17 immune response in psoriasis, accompanied by selective reduction of ω3 PUFA metabolites.

Attenuated Psoriasis and CHS in Pla2g2d-TG Mice—To obtain additional evidence for the immunosuppressive function of sPLA₂-IID, we generated *Pla2g2d*-overexpressing TG mice in accordance with the procedure depicted in Fig. 3*A* (for details, see "Experimental Procedures"). An example of PCR genotyping is shown in Fig. 3*B*. As a result of the *Cre/loxP* reac-
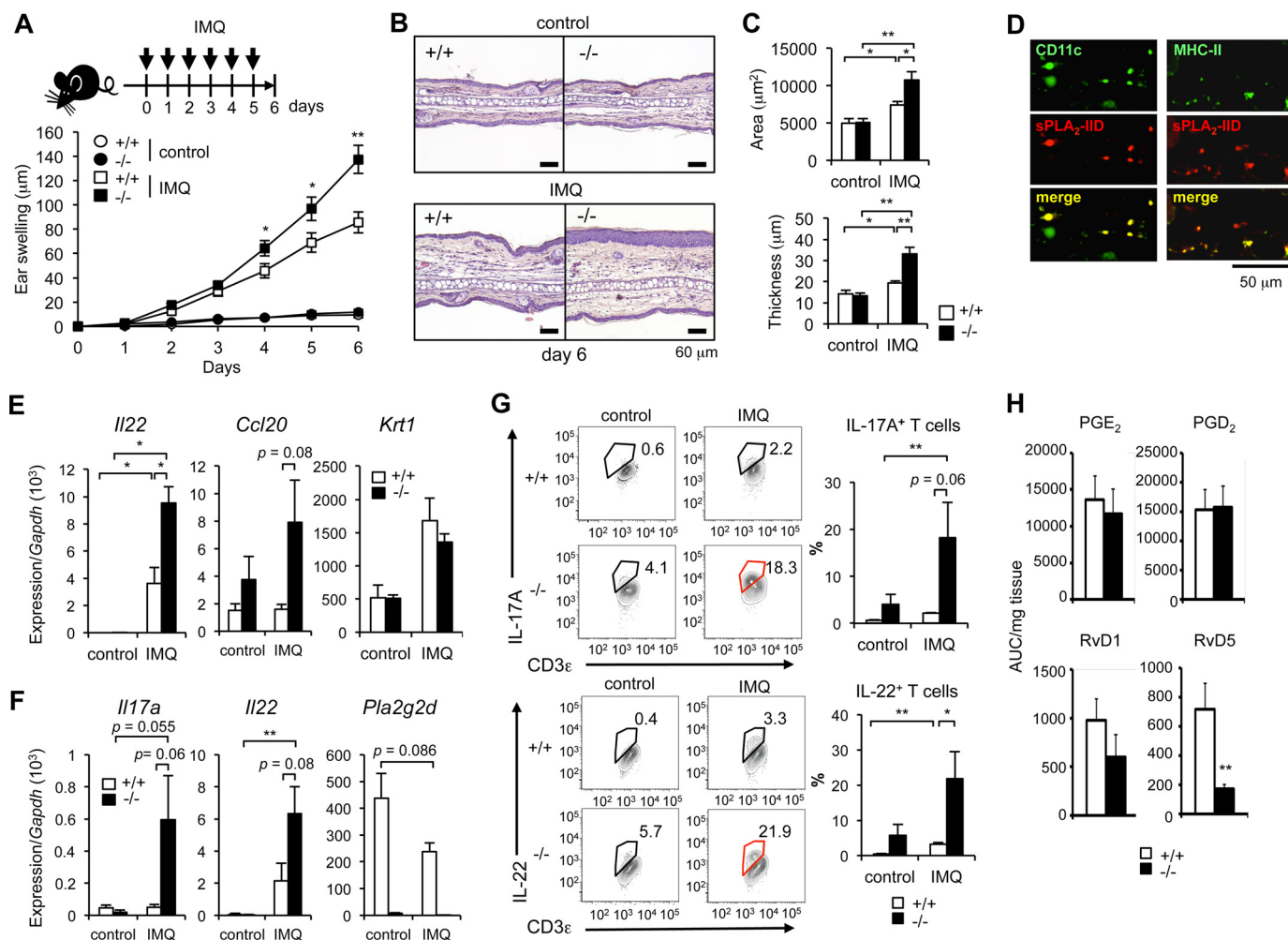
FIGURE 2. **Exacerbation of IMQ-induced psoriasis in *Pla2g2d*$^{-/-}$ mice.** *A,* schematic representation of the procedure (*top panel*) and the kinetics of ear swelling in *Pla2g2d*$^{+/+}$ and *Pla2g2d*$^{-/-}$ mice with or without IMQ treatment for the indicated periods (*n* = 20) (*bottom panel*). *B,* ear histology in *Pla2g2d*$^{+/+}$ and *Pla2g2d*$^{-/-}$ mice with or without IMQ treatment for 6 days. *C,* evaluations of the area (*top panel*) and thickness (*bottom panel*) of *Pla2g2d*$^{+/+}$ and *Pla2g2d*$^{-/-}$ epidermis on day 6 (*n* = 5). *D,* confocal immunofluorescence of sPLA₂-IID (*red*), DC markers (CD11c and MHC-II; *green*), and their merged images in IMQ-treated WT mice on day 6. *E* and *F,* expression of various genes in the skin (*E*) and LNs (*F*) of *Pla2g2d*$^{+/+}$ and *Pla2g2d*$^{-/-}$ mice on day 6, with *Gapdh* as a normalization control (*n* = 3–4). *G,* flow cytometry of IL-17A- or IL-22-expressing T cells in the skin of *Pla2g2d*$^{+/+}$ and *Pla2g2d*$^{-/-}$ mice on day 6 (*n* = 3), with representative FACS profiles (*left*). *H,* ESI-MS analysis of AA-derived PGs and DHA-derived Rvs in the skin of IMQ-treated *Pla2g2d*$^{+/+}$ and *Pla2g2d*$^{-/-}$ mice on day 6 (*n* = 8). Values are mean ± S.E., *, *p* < 0.05, and **, *p* < 0.01. *B* and *D,* representative images in two independent experiments are shown.

tion, the amplified fragment for the *Pla2g2d* transgene shifted from a 1,300-bp band (for silent *LNL-Pla2g2d*) to a 170-bp band (for active *Pla2g2d*). *Pla2g2d* expression in various tissues as well as in bone marrow-derived macrophages and DCs was markedly higher in *Pla2g2d*-TG mice than in control mice (Fig. 3*C*). In the LNs, the steady-state levels of ω3 PUFA metabolites were consistently (>2-fold) elevated in *Pla2g2d*-TG mice compared with WT mice, although the levels of some ω6 AA-derived metabolites also tended to be slightly higher in the TG mice (Fig. 3*D*). *Pla2g2d*-TG mice were born normally and were fertile, showing normal serum biochemical parameters over 6 months under normal housing conditions.

We then subjected *Pla2g2d*-TG mice and littermate WT mice to the models of psoriasis (Fig. 4, *A–F*) and CHS (Fig. 4, *G* and *H*). In sharp contrast to *Pla2g2d*$^{-/-}$ mice (Fig. 2), IMQ-induced ear swelling was significantly ameliorated in *Pla2g2d*-TG mice compared with WT mice (Fig. 4*A*). In both skin and LNs, *Pla2g2d* expression was markedly higher in *Pla2g2d*-TG mice than in WT mice, irrespective of IMQ

challenge (Fig. 4*B*). The LN expression of *Il17a* and *IL-22* was substantially lower in IMQ-treated *Pla2g2d*-TG mice than in replicate WT mice (Fig. 4*C*). This observation was further supported by flow cytometry, where the IMQ-induced increase in IL-17A- or IL-22-expressing CD3ε$^+$ T cells was significantly reduced in *Pla2g2d*-TG skin relative to WT skin (Fig. 4, *D* and *E*). Furthermore, the skin level of RvD1 was substantially higher in IMQ-treated *Pla2g2d*-TG mice than in WT mice (Fig. 4*F*).

In the elicitation phase of CHS, *Pla2g2d* ablation results in delayed resolution of Th1-driven dermatitis (12). Conversely, DNFB-challenged *Pla2g2d*-TG mice displayed an earlier recovery from ear swelling than did replicate WT mice, although progression of the edema during the initial 2 days was comparable between the genotypes (Fig. 4*G*). Moreover, on day 5, skin expression of inflammatory markers, including *Ifng, S100a9, Itgax,* and *Itgam,* was consistently lower in *Pla2g2d*-TG mice than in WT mice (Fig. 4*H*). These results fully reciprocate the CHS phenotypes observed in *Pla2g2d*$^{-/-}$ mice (12) and sub-
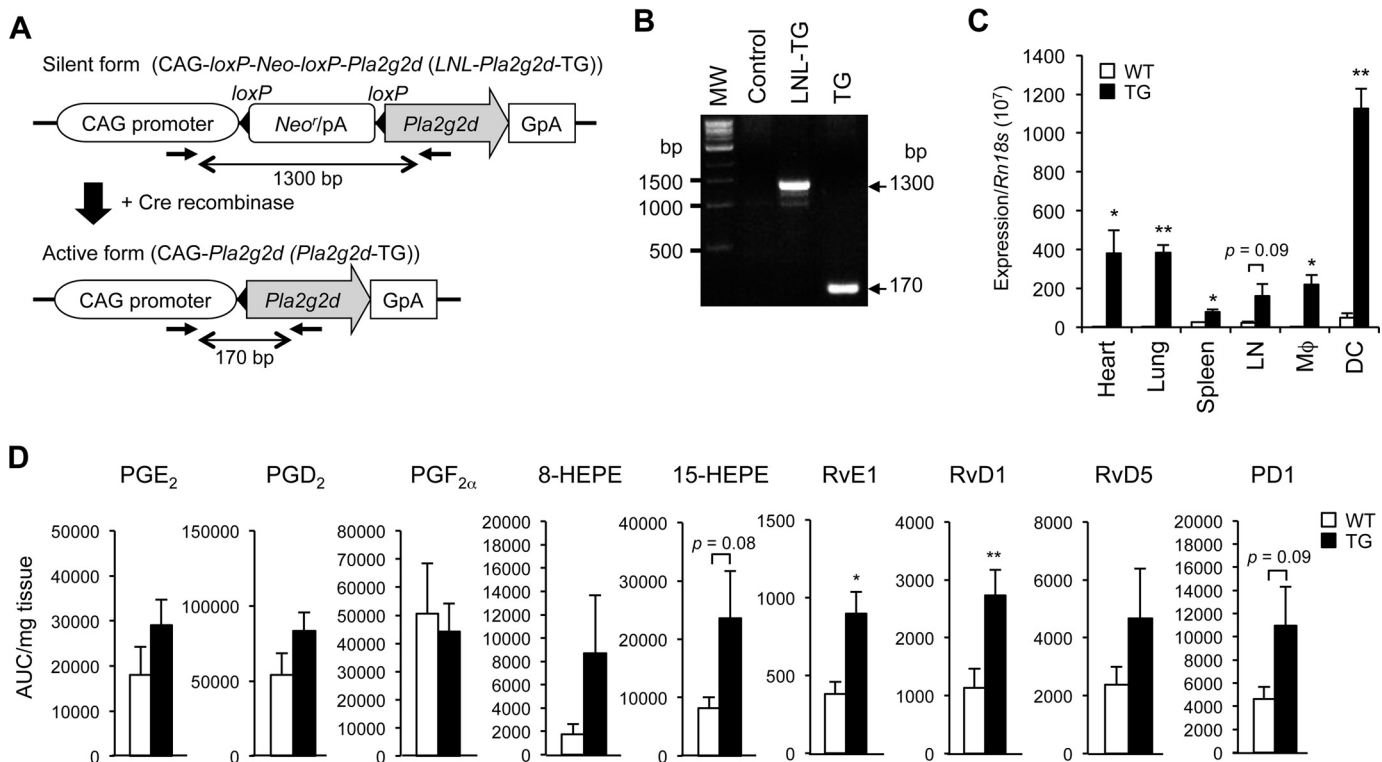
FIGURE 3. **Increased ω3 PUFA metabolite levels in the LNs of *Pla2g2d*-TG mice.** *A,* generation of *Pla2g2d*-TG mice. Details of the procedure are described under "Experimental Procedures." *B,* representative PCR genotyping of WT control, *LNL-Pla2g2d*-TG, and *Pla2g2d*-TG mice. *MW,* molecular weight. *C,* quantitative RT-PCR of *Pla2g2d* relative to *Rn18s* in various tissues and cells of *Pla2g2d*-TG and WT mice ($n = 3$). *D,* ESI-MS analysis of various lipids in the LNs of *Pla2g2d*-TG and WT mice ($n = 9-10$). Values are mean $\pm$ S.E., *, $p < 0.05$, and **, $p < 0.01$.

stantiate the notion that sPLA₂-IID has an immunosuppressive role in various types of immune responses.

Effects of PUFAs and Their Metabolites on Th17-type Immunity in Primary Culture—Next, we used bone marrow-derived DCs (BMDCs) and primary LN cells in *ex vivo* culture to assess the roles of sPLA₂-IID and its potential lipid products in the Th17-type immune response in the context of psoriasis. After a 6-h stimulation with IMQ, an agent that induces the psoriasis-like Th17 response (see above), expression of *Il6* and *Il23a* was induced more robustly in *Pla2g2d*$^{-/-}$ DCs than in *Pla2g2d*$^{+/+}$ DCs (Fig. 5A). Additionally, *Pla2g2d*$^{-/-}$ DCs expressed more *Il12a* (a Th1 cytokine) than did *Pla2g2d*$^{+/+}$ DCs at each time point regardless of IMQ treatment (Fig. 5A), suggesting that sPLA₂-IID alleviates the Th1 immunity even under the basal state.

When WT-derived BMDCs were stimulated with IMQ in the presence of various lipids, the expression of *Il6* and *Il23a* was reduced modestly by ω3/ω6 PUFAs and markedly by several ω3 eicosapentaenoic acid (EPA) and DHA metabolites, including 18-hydroxy-EPA, RvD1, RvD2 (7,16,17-trihydroxy-DHA), protectin D1 (10,17-dihydroxy-DHA), and 10-hydroxy-DHA, whereas AA metabolites, including several PGs, leukotriene B₄, and lipoxin A₄ (LXA₄), failed to affect their expression significantly (Fig. 5B). Although EPA-derived RvE1 (5,12,18-trihydroxy-EPA) had no significant effects on the expression of *Il6* and *Il23a* (Fig. 5B), it significantly increased that of *Il10*, an anti-inflammatory cytokine, in BMDCs (Fig. 5C). Expression of the psoriasis-related cytokines *Tnf* and *Il22* in IMQ-treated LN cells was reduced to varying degrees by various AA, EPA, and

DHA metabolites as well as by DHA itself, whereas AA and EPA modestly enhanced the expression of *Il22* (Fig. 5D). Furthermore, RvD1, rather than its precursor DHA, reduced the secretion of IL-17A protein by IMQ-stimulated LN cells (Fig. 5E). Thus, although the effects of various PUFAs and their metabolites were not entirely identical and appeared to depend on the experimental conditions or cellular sources employed, it is likely that several ω3 (and even ω6) PUFA metabolites have the capacity to potently block the Th17-driven inflammatory response.

sPLA₂-IID Exacerbates Skin Cancer by Attenuating Anti-tumor Immunity—The aforementioned results, together with those of our previous study (12), suggest that sPLA₂-IID attenuates various types of inflammatory response (LN inflammation in irritant dermatitis, Th1-driven CHS, and Th17-driven psoriasis) through the production of pro-resolving lipid metabolites. However, this beneficial immunosuppressive property of sPLA₂-IID is conversely disadvantageous in certain situations such as host defense, as demonstrated by the finding that sPLA₂-IID suppresses an anti-viral Th1 immune response, leading to increased coronavirus infection and thereby augmented lung inflammation (28). We therefore speculated that, as in the case of anti-viral immunity, sPLA₂-IID might prevent anti-tumor immunity, thereby promoting tumor development.

To this end, we applied a model of chemical carcinogenesis induced by 9,10-dimethylbenz(*a*)anthracene (DMBA) and 12-O-tetradecanoylphorbol-13-acetate (TPA) to *Pla2g2d*$^{-/-}$ mice and littermate WT mice on a BALB/c background, a strain that is sensitive to this model (a schema of the procedure is
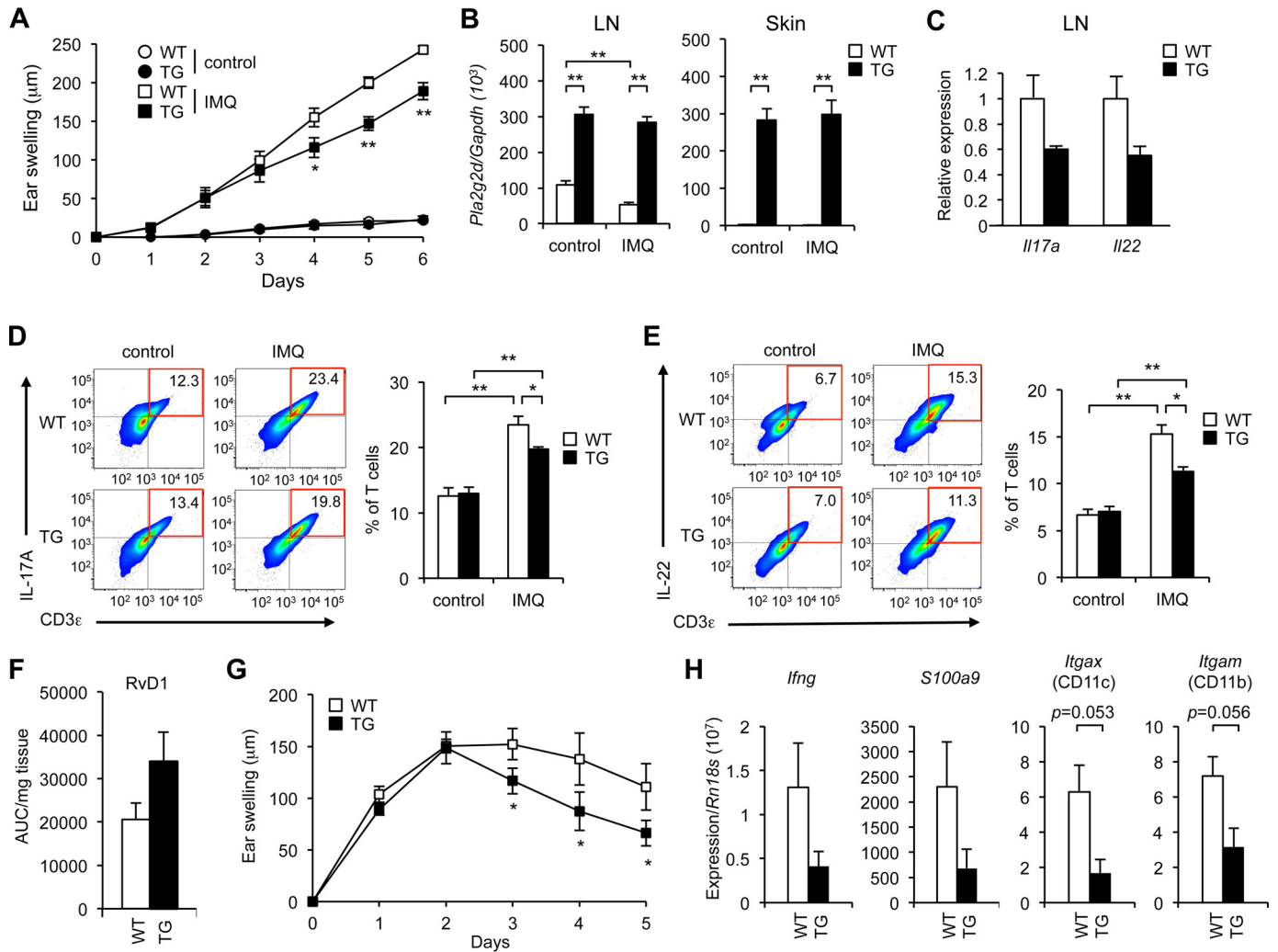
FIGURE 4. **Attenuated psoriasis and CHS in *Pla2g2d*-TG mice.** *Pla2g2d*-TG and littermate WT mice were subjected to the psoriasis (*A–F*) and CHS models (*G* and *H*). *A*, time course of ear swelling in *Pla2g2d*-TG and WT mice with or without IMQ treatment for the indicated periods (*n* = 9–16). *B*, quantitative RT-PCR of *Pla2g2d* relative to *Gapdh* in the LNs and skin of *Pla2g2d*-TG and WT mice with or without IMQ treatment for 6 days (*n* = 3–4). *C*, quantitative RT-PCR of Th17 cytokines in the LNs and skin of *Pla2g2d*-TG and WT mice treated with IMQ for 6 days, the expression in WT being regarded as 1 (*n* = 3–4). *D* and *E*, flow cytometry of T cells expressing IL-17A (*D*) or IL-22 (*E*) in the skin of *Pla2g2d*-TG and WT mice with or without IMQ treatment for 6 days (*n* = 4), with representative FACS profiles (*left*). *F*, ESI-MS analysis of the RvD1 level in the skin of *Pla2g2d*-TG and WT mice treated with IMQ for 6 days (*n* = 3–4). *G*, time course of ear swelling in *Pla2g2d*-TG and WT mice that were sensitized with DNFB on day −5 and then re-challenged with DNFB for the indicated periods (*n* = 16). *H*, quantitative RT-PCR of inflammatory markers in the skin of *Pla2g2d*-TG and WT mice on day 5 after DNFB re-challenge, with *Rn18s* as a normalization control (*n* = 3). Values are mean ± S.E., *, $p < 0.05$, and **, $p < 0.01$.

depicted in Fig. 6*A*). At 24 weeks, *Pla2g2d*$^{-/-}$ mice were highly protected from the development of skin tumors (Fig. 6*B*). Tumor incidence and multiplicity over time were delayed (Fig. 6, *C* and *D*), and the average tumor volume at 24 weeks was apparently small (Fig. 6*E*) in *Pla2g2d*$^{-/-}$ mice relative to *Pla2g2d*$^{+/+}$ mice. Among the knock-out mouse lines for several sPLA₂s, the significant reduction of tumor development was evident in *Pla2g2d*$^{-/-}$ (tumor weight and number) and *Pla2g2f*$^{-/-}$ (tumor weight) mice but not in *Pla2g2e*$^{-/-}$, *Pla2g5*$^{-/-}$, and *Pla2g10*$^{-/-}$ mice (Fig. 6, *F* and *G*). The protection of *Pla2g2f*$^{-/-}$ mice against skin cancer was ascribed to decreased keratinocyte hyper-growth by the absence of epidermal sPLA₂-IIF, as we have reported recently (24).

At 4 weeks, an early time point when papillomas were still not apparent, the DMBA/TPA-induced epidermal thickening was already milder in *Pla2g2d*$^{-/-}$ mice than in *Pla2g2d*$^{+/+}$ mice (Fig. 7, *A* and *B*). Notably, the expression of *Arg1* and *Cd206*,

markers for tumor-promoting M2-like macrophages (34), but not *Cd68*, a marker for tumor-suppressing M1-like macrophages, was substantially lower in *Pla2g2d*$^{-/-}$ skin than in *Pla2g2d*$^{+/+}$ skin at 4 weeks after DMBA/TPA treatment (Fig. 7*C*). Consistent with this, flow cytometry of splenic (Fig. 7*D*) and LN (data not shown) cells revealed a reduction of M2-like macrophages (CD11c^{lo}CD206^{hi}) and an increase of M1-like macrophages (CD11c^{hi}CD206^{lo}) in *Pla2g2d*$^{-/-}$ mice than in *Pla2g2d*$^{+/+}$ mice even under the steady-state condition. Quantitative RT-PCR of the regional LNs further confirmed the lower expression of the M2-like macrophage marker *Arg1* in *Pla2g2d*$^{-/-}$ mice than in *Pla2g2d*$^{+/+}$ mice in both control and disease settings (Fig. 7*E*). In addition, CD8α^+IFN-γ^+ T cells in the regional LNs tended to be more abundant in DMBA/TPA-treated *Pla2g2d*$^{-/-}$ mice than in replicate *Pla2g2d*$^{+/+}$ mice (Fig. 7*F*). Moreover, the steady-state levels of RvD2 and maresin 1, which are DHA-derived lipid mediators that promote M2
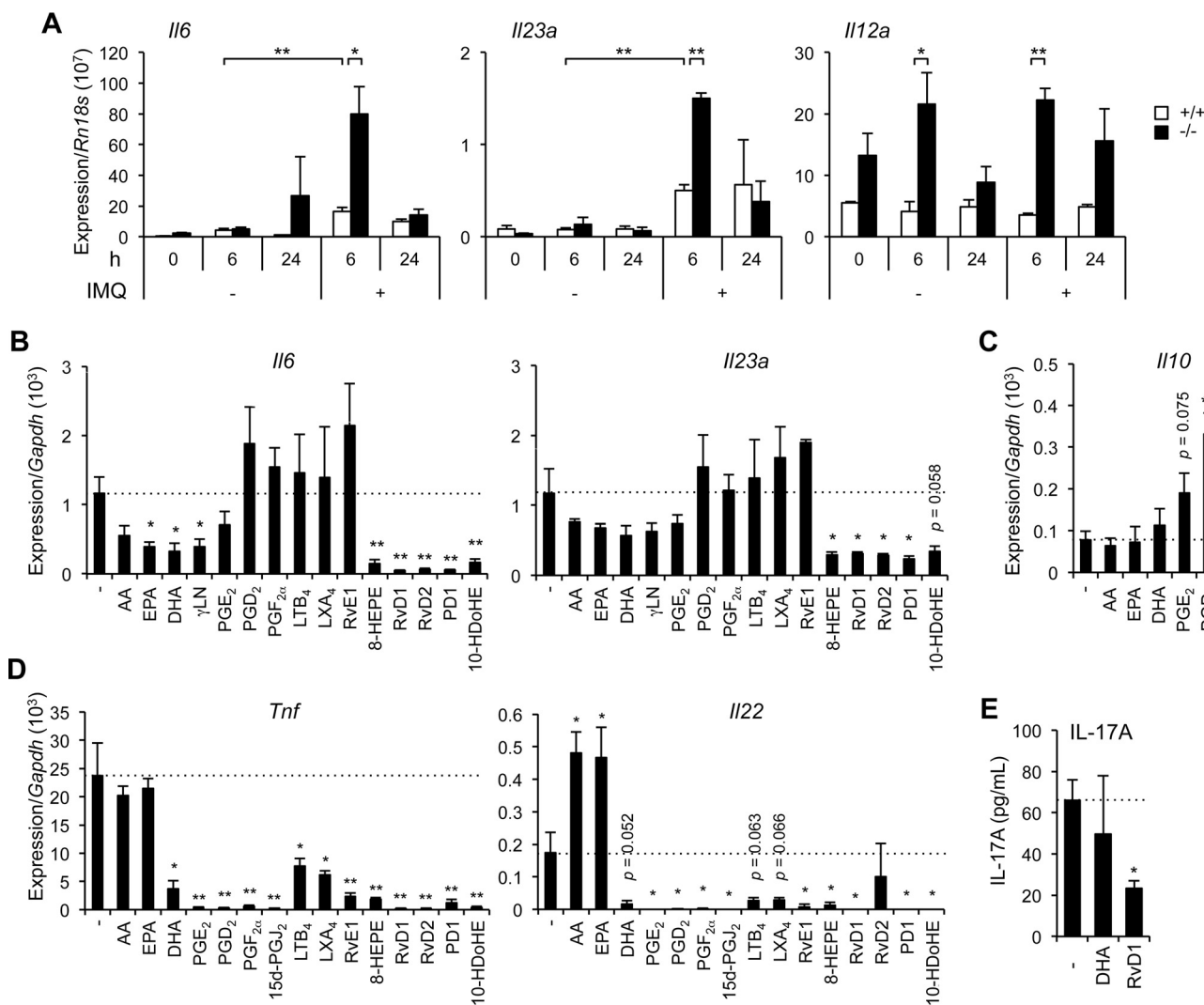
FIGURE 5. **Effects of PUFAs on Th1/Th17 cytokine expression in DCs and LN cells.** *A,* quantitative RT-PCR of cytokines in BMDCs from *Pla2g2d$^{+/+}$* and *Pla2g2d$^{-/-}$* mice after stimulation for the indicated periods with (+) or without (−) IMQ (n = 3). *B–D,* quantitative RT-PCR (*B–D*) or ELISA (*E*) of cytokines in BMDCs (*B* and *C*) or LN cells (*D* and *E*) after stimulation for 6 h with IMQ in the presence or absence (−) of the indicated lipids (10 nM) (n = 5). *Dashed lines* in *B–E* indicate the expression level of each cytokine without addition of lipids. In quantitative RT-PCR, values are normalized with *Rn18s* (*A*) or *Gapdh* (*B–D*). Values are mean ± S.E. *, $p < 0.05$, and **, $p < 0.01$. γLN, γ-linolenic acid; *15d-PGJ₂*, 15-deoxy-PGJ₂.

macrophage polarization (40–45), were reduced in the LNs of *Pla2g2d$^{-/-}$* mice compared with *Pla2g2d$^{+/+}$* mice (Fig. 7G). This difference was not seen in the DMBA/TPA-treated group as the levels of these lipid mediators in *Pla2g2d$^{+/+}$* mice were decreased to their levels in *Pla2g2d$^{-/-}$* mice, most likely due to down-regulation of *Pla2g2d* expression (see above). These results suggest that the absence of sPLA₂-IID results in augmentation of anti-tumor immunity by decreasing tumor-promoting M2-like macrophages and increasing tumor-suppressing M1-like macrophages and cytotoxic T cells.

We then applied *Pla2g2d*-TG mice (C57BL/6 background) to the DMBA/TPA-induced skin carcinogenesis model. Beyond the limitation that the C57BL/6 strain is relatively insensitive to this model, constitutive expression of *Arg1* was elevated (Fig. 7H) and DNBA/TPA-induced expression of *Ifng* was dampened (Fig. 7I) in *Pla2g2d*-TG skin compared with WT skin. Thus, as opposed to *Pla2g2d* deficiency, its TG overexpression shifts the immune balance toward suppression of the anti-tumor immunity.

Discussion

Impairment of the counter-regulatory pathways against pro-inflammatory immune responses is often detrimental and results in various diseases associated with chronic inflammation. With regard to the mechanisms underlying the effect of ω3 PUFAs on resolution mediator networks, it has been considered that resolvins and protectins, a family of ω3 PUFA-derived local mediators with unique anti-inflammatory activities and temporal profiles, occupy a position between the early response to inflammatory challenge and the resolution pathways where the initiating programs signal the termination (7, 35). As our understanding of the pro-resolving lipid mediator pathways has increased, there has been an emerging interest in the roles of PLA₂s that can supply ω3 PUFAs upstream of their biosynthetic conversion to pro-resolving lipid mediators. Our recent efforts to clarify the biological functions of various PLA₂s using knockout and/or transgenic strategies in combination with comprehensive lipidomics approaches have shown that two particular
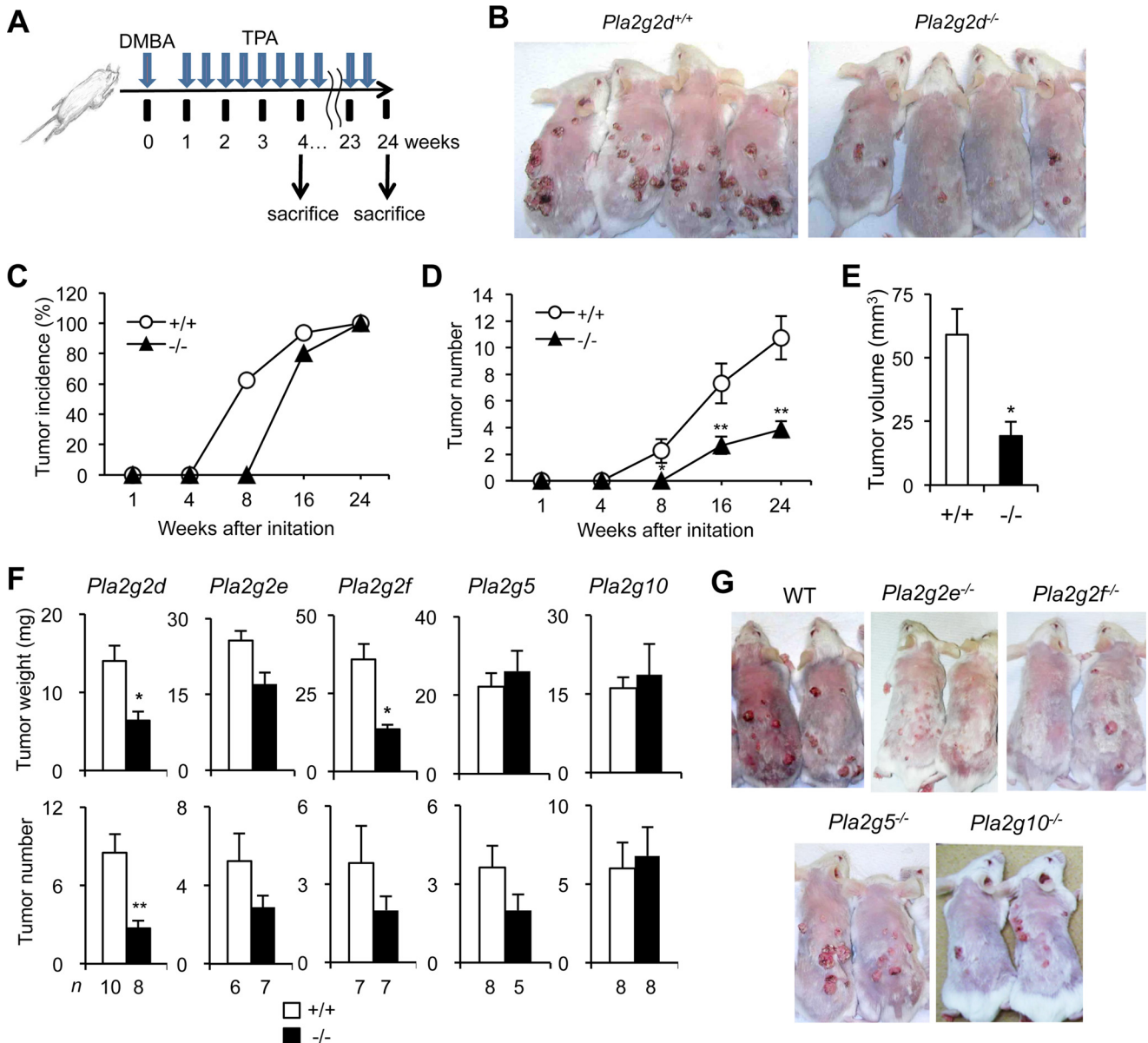
FIGURE 6. **Reduced skin carcinogenesis in *Pla2g2d$^{-/-}$* mice.** *A,* schematic representation of the procedure for DMBA/TPA-induced skin cancer. *B,* gross appearances of *Pla2g2d$^{+/+}$* and *Pla2g2d$^{-/-}$* mice at 24 weeks. *C* and *D,* monitoring of tumor incidence (*C*) and numbers (*D*) in DMBA/TPA-treated *Pla2g2d$^{+/+}$* and *Pla2g2d$^{-/-}$* skins at various time points ($n = 12$). *E,* average tumor volumes in DMBA/TPA-treated *Pla2g2d$^{+/+}$* and *Pla2g2d$^{-/-}$* skins at 24 weeks ($n = 12$). *F* and *G,* tumor weights (*upper panels*) and numbers (*bottom panels*) in various sPLA$_2$ knock-out mice and their littermate controls at 24 weeks (*F*). Representative images of gross appearances are shown (*G*). Values are mean ± S.E. *, $p < 0.05$, and **, $p < 0.01$.

sPLA$_2$s in specific locations, *i.e.* sPLA$_2$-IID in lymphoid DCs and sPLA$_2$-X in the colorectal epithelium, do mobilize ω3 PUFAs *in vivo*, thereby protecting against delayed-type hypersensitivity and colitis, respectively (12, 14).

Our recent study has demonstrated that sPLA$_2$-IID, a DC-expressed "resolving sPLA$_2$," retards the resolution of Th1-driven inflammation in the skin and draining LNs by preferentially mobilizing DHA-derived pro-resolving lipid mediators (12). To gain further insights into the function of sPLA$_2$-IID, we have herein extended our study to other disease models using *Pla2g2d$^{-/-}$* mice as well as newly generated *Pla2g2d*-TG mice and obtained evidence that sPLA$_2$-IID ameliorates various types of immune response in general, including LN inflammation in acute irritant dermatitis, Th1-dependent CHS, and

Th17-dependent psoriasis. This function could be explained, at least partly, by the ability of sPLA$_2$-IID to mobilize ω3 PUFA metabolites that dampen the Th1- or Th17-type immune responses. The lack of sPLA$_2$-IID markedly reduces the steady-state levels of ω3 PUFAs and their metabolites and skews macrophages toward an M1-like subtype in lymphoid tissues, suggesting that the constitutive supply of ω3 PUFA metabolites by this sPLA$_2$ may put a brake on the ongoing DC-driven acquired immunity.

In contrast to its suppressive roles in CHS and psoriasis, sPLA$_2$-IID accelerates the development of skin tumors, probably because this enzyme attenuates anti-tumor Th1 immunity. This is reminiscent of the role of sPLA$_2$-IID in host defense against viral infection, where the reduction of anti-viral Th1
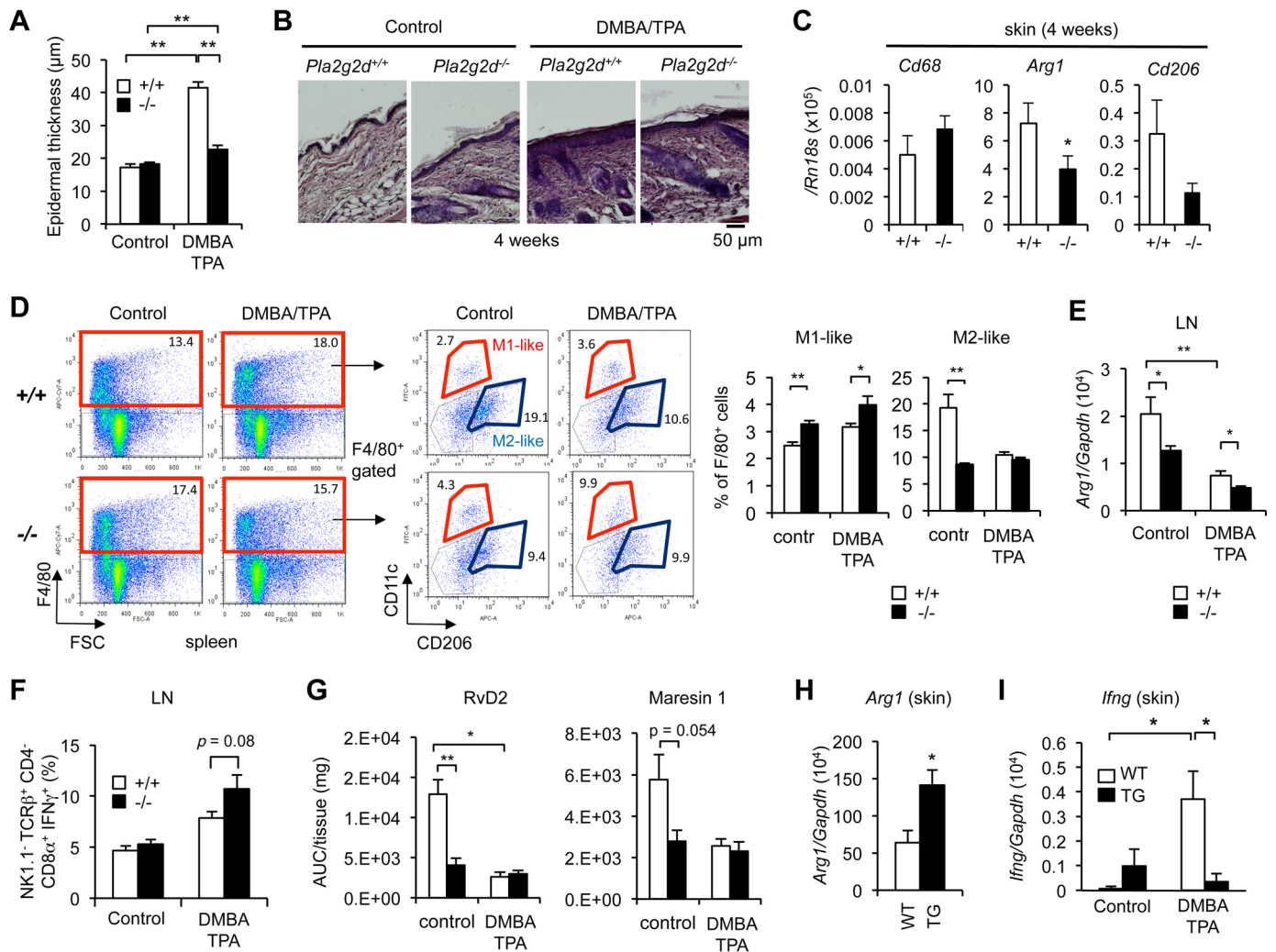
FIGURE 7. **sPLA$_2$-IID augments anti-tumor immunity.** *A* and *B,* epidermal thickness ($n = 3$) (*A*) and representative hematoxylin/eosin staining (*B*) of skin sections from *Pla2g2d$^{+/+}$* and *Pla2g2d$^{-/-}$* mice with or without DMBA/TPA treatment at 4 weeks. *C,* quantitative RT-PCR of macrophage markers in DMBA/TPA-treated *Pla2g2d$^{+/+}$* and *Pla2g2d$^{-/-}$* skins at 4 weeks, with *Rn18s* as a normalization control ($n = 6$). *D,* flow cytometry of M1- or M2-like macrophages in the spleen of *Pla2g2d$^{+/+}$* and *Pla2g2d$^{-/-}$* mice with or without DMBA/TPA treatment for 4 weeks ($n = 7$), with representative FACS profiles in which F4/80-positive cells were sorted for expression of CD11c (M1) or CD206 (M2). *E–G,* quantitative RT-PCR of *Arg1* (*E*), flow cytometry of cytotoxic T cells (*F*), and lipidomics detection of RvD2 and maresin 1 (*G*) in the LNs of *Pla2g2d$^{+/+}$* and *Pla2g2d$^{-/-}$* mice with or without DMBA/TPA treatment for 4 weeks ($n = 7$). *H* and *I,* quantitative RT-PCR of *Arg1* (*H*) and *Ifng* (*I*) in the skin of *Pla2g2d*-TG and WT mice with or without DMBA/TPA treatment for 4 weeks ($n = 4$–8). Values are mean $\pm$ S.E. *, $p < 0.05$, and **, $p < 0.01$.

immunity through the action of this sPLA$_2$ increases the infection and eventually worsens pulmonary inflammation (28). Given that some ω3 PUFA metabolites facilitate M2 polarization of macrophages (36, 37), our observations suggesting that tumor-associated M2-like macrophages, which promote cancer progression by releasing a panel of factors that prevent the recruitment or functions of cytotoxic T and NK cells (34), are reduced in *Pla2g2d$^{-/-}$* mice and conversely increased in *Pla2g2d*-TG mice also fit with the current view. Thus, the immunosuppressive function of sPLA$_2$-IID provides favorable or unfavorable outcomes in distinct disease settings, thereby protecting against inflammation and exacerbating infection and cancer.

Reportedly, ectopic administration of ω3 PUFA metabolites (38–40) or systemic overproduction of these lipids in mice transgenic for *Fat-1* (an ω3 PUFA synthase in *Caenorhabditis elegans*) (41) confers protective effects against infection-based inflammation or cancer xenograft by facilitating phagocytotic clearance of hazardous materials by innate immune cells such as neutrophils and macrophages. Apart from this systemic effect of ω3 PUFAs, the spatiotemporal supply of ω3 PUFAs by sPLA$_2$-IID, which is expressed preferentially and constitutively in DCs in local niches (particularly those in lymph tissues), may exert a distinct impact on acquired immunity by suppressing the functions of DCs, T cells, or their interactions. Indeed, multiple ω3 PUFA metabolites could attenuate the production of cytokines crucial for Th1/Th17 responses (this study) and reduce the migration or activation of DCs (12, 13, 28) and the functions of T and B cells (42, 43). Although the molecular basis underlying the actions of individual ω3 PUFA metabolites still remains elusive, it is tempting to speculate that they may exert their specific functions by acting on distinct receptors or through other mechanisms in different target cells. In this regard, the proposed mechanistic actions of ω3 PUFA metabolites include specific signaling through lipid-sensing receptors (9, 10, 44, 45), attenuation of lipotoxicity-induced endoplasmic

reticulum stress (46), and an increase in membrane fluidity leading to alterations of transmembrane or intracellular signaling (47), among others. In fact, ω3 PUFAs themselves can block Th17 cytokine production by lamina propria lymphocytes in colitis (14) and inflammasome activation in obesity (48–50) through the fatty acid receptor GPR40 or GPR120.

Nonetheless, the possibility that sPLA$_2$-IID exerts its anti-inflammatory function through mobilization of other lipids, including certain ω6 PUFA-derived metabolites or lysophospholipids that were not tested in this study, cannot be fully ruled out. Indeed, sPLA$_2$-IID appears to be coupled with the AA-PGD$_2$-DP1 axis in the lung LNs during pulmonary viral infection (28). Also, some lysophospholipid species, such as lysophosphatidylserine, have anti-inflammatory effects on innate and acquired immune responses through specific receptors (51, 52). Whether the immunosuppressive function of sPLA$_2$-IID could be linked to the generation of these anti-inflammatory lipids under particular disease conditions remains to be elucidated and requires further investigations.

The dual roles of sPLA$_2$s in promoting or attenuating diseases may be dictated by the cells they are secreted from, the target membranes they act on, the types of lipid metabolites they generate, or when and how these lipid metabolites are linked to particular biological processes in cell-, tissue-, or disease-specific contexts. For instance, sPLA$_2$-IIA, a prototypic sPLA$_2$ isoform that is inducible by pro-inflammatory stimuli, amplifies sterile inflammation by hydrolyzing membranes in microparticles, particularly extracellular mitochondria (53), whereas it has a protective effect against infection-induced inflammation such as sepsis and pneumonia by degrading membranes in invading bacteria (54). sPLA$_2$-V, which is induced by Th2 cytokines or metabolic stress, promotes M2 macrophage polarization and Th2 immunity by altering the local balance of unsaturated *versus* saturated fatty acids or by facilitating phagocytosis of harmful components, thereby aggravating Th2-driven asthma and attenuating Th1/Th17-related anti-fungal defense, arthritis, and obesity (23, 26, 27, 55, 56). sPLA$_2$-X exacerbates asthma by mobilizing AA metabolites in the lung (25), while protecting against colitis by mobilizing ω3 PUFAs in the colon (14). From these standpoints, sPLA$_2$-IID represents another example of the "good" and "bad" faces of this extracellular lipolytic enzyme family, by spatiotemporally supplying ω3 PUFAs in local tissue microenvironments where DC-driven acquired immunity plays fundamental roles in inflammation or in host defense against infection and cancer.

Overall, our current studies point to potential prophylactic or therapeutic use of an agent that would specifically stabilize or inhibit sPLA$_2$-IID according to disease contexts. Nonetheless, targeting sPLA$_2$-IID, as well as other sPLA$_2$s in general, will be a challenge, because these enzymes appear to play highly selective and often opposite roles in specific organs and disease states.

Experimental Procedures

Mice—All mice were housed in climate-controlled (23 °C) specific pathogen-free facilities with a 12-h light-dark cycle, with free access to standard laboratory food (CE2 Laboratory Diet, CLEA, Japan) and water. $Pla2g2d^{-/-}$, $Pla2g2e^{-/-}$, $Pla2g2f^{-/-}$, $Pla2g5^{-/-}$, and $Pla2g10^{-/-}$ mice and their littermate controls, backcrossed to C57BL/6 or BALB/c mice (Japan SLC) for more than 12 generations, were described previously (12, 14, 22–24). All animal experiments were performed in accordance with protocols approved by the Institutional Animal Care and Use Committees of the Tokyo Metropolitan Institute of Medical Science in accordance with the Japanese Guide for the Care and Use of Laboratory Animals.

Generation of Pla2g2d-TG Mice—The strategy for generation of sPLA$_2$-overexpressing TG mice has been reported previously (57). In brief, mouse *Pla2g2d* cDNA was inserted into the EcoRI site (downstream of the *CAG* (cytomegalovirus immediate early enhancer-chicken β-actin hybrid) promoter) in the pCALNL5 vector (Fig. 3A) (58). The plasmid, containing the transgene downstream of a neomycin cassette (*Neo^r*) with *LoxP* sites at both ends, was excised at the HindIII and SalI sites to produce a 6-kb *CAG-LoxP-Neo^r-LoxP-Pla2g2d* (*LNL-Pla2g2d*) fragment. Then the DNA was injected into fertilized eggs. Genotyping was performed on genomic DNA from tail biopsies by PCR using the primer pairs 5′-TGGTTATTGT-GCTGTCTCATCATTT-3′ and 5′-GGCTTTCTTCCCCGT-CATGTGT-3′ (Sigma Genosys), which amplified a 1,300-bp fragment specific for *LNL-Pla2g2d*. The reaction was conducted at 95 °C for 10 s and then 35 cycles at 95 °C for 0 s and 65 °C for 1 min on an Applied Biosystems 9800 Fast Thermal Cycler (Applied Biosystems). The PCR products were analyzed by 1.5% (w/v) agarose gel electrophoresis with ethidium bromide. Male founders were mated with female C57BL/6 mice to confirm germ line transmission by PCR genotyping, and those with successful germ line transmission (*LNL-Pla2g2d*-TG) were then crossed with female *CAG-Cre$^{tg/+}$* mice, which carry a Cre recombinase transgene under control of the *CAG* promoter (58). This step resulted in removal of the *Neo^r* cassette from the *LNL-Pla2g2d* transgene, thereby allowing activation of the *Pla2g2d* transgene in the whole body of the offspring. *Pla2g2d*-TG mice were inbred with C57BL/6 mice. Phenotypes that appeared in *Pla2g2d*-TG mice, which carried the active *Pla2g2d* transgene, but not in *LNL-Pla2g2d*-TG mice, in which the *Pla2g2d* transgene remained silent, were regarded as events caused by the overexpressed sPLA$_2$-IID.

Quantitative RT-PCR—Total RNA was extracted from tissues and cells using TRIzol reagent (Invitrogen). First-strand cDNA synthesis was performed using a high capacity cDNA reverse transcriptase kit (Applied Biosystems). PCRs were carried out using a Power SYBR Green PCR system (Applied Biosystems) or a TaqMan Gene Expression System (Applied Biosystems) on the ABI7300 Quantitative PCR system (Applied Biosystems). The probe/primer sets used are listed in Table 1.

Histological Analysis—Histological analysis was performed as described previously (12). In brief, mouse tissues were fixed with 100 mM phosphate buffer (pH 7.2) containing 4% (w/v) paraformaldehyde, embedded in paraffin, sectioned, mounted on glass slides, deparaffinized in xylene, and rehydrated in ethanol with increasing concentrations of water. Hematoxylin and eosin staining was performed on the 5-μm-thick cryosections, and the stained sections were analyzed using a BX61 microscope (Olympus). Epidermal layer thickness was measured using DP2-BSW software (Olympus).

TABLE 1
List of primers used in quantitative RT-PCR

Gene	Accession number	Forward Primer	Reverse Primer	Probe Number (Roche)
Ccl2	NM_011333.3	5'-catccacgtgttggctca-3'	5'-gatcatcttgctggtgaatgagt-3'	62
Ccl19	NM_011888.2	5'-tgtggcctgcctcagattat-3'	5'-agtcttccgcatcattagcac-3'	40
Ccl20	NM_016960.2	5'-aactgggtgaaaagggctgt-3'	5'-gtccaattccatcccaaaaa-3'	73
Ccr5	NM_009917.5	5'-gagacatccgttccccctac-3'	5'-gtcggaactgacccttgaaa-3'	106
Ccr7	NM_007719.2	5'-ctccttgtcatttttccaggtg-3'	5'-tggtattctcgccgatgtagt-3'	29
Ifng	NM_008337.1	5'-atctggaggaactggcaaaa-3'	5'-ttcaagacttcaaagagtctgaggta-3'	21
Il6	NM_031168.1	5'-gctaccaaactggatataatcagga-3'	5'-ccaggtagctatggtactccagaa-3'	6
Il12a	NM_008351.1	5'-atcacaaccatcagacagatca-3'	5'-cgccattatgattcagagactg-3'	49
Il17a	NM_010552.2	5'-cagggagagcttcatctgtgt-3'	5'-gctgagctttgagggatgat-3'	74
Il22	NM_016971.1	5'-ttcctgaccaaactcagca-3'	5'-ctggatgttctggtcgtcac-3'	17
Il23a	NM_031252.2	5'-tccctactaggactcagccaac-3'	5'-agaactcaggctgggagcatc-3'	19
Itgam	NM_001082960.1	5'-caatagccagcctcagtgc-3'	5'-gagcccaggggagaagtg-3'	76
Itgax	NM_021334.2	5'-atggagcctcaagacaggac-3'	5'-ggatctgggatgctgaaatc-3'	20
Krt1	NM_008473.2	5'-tttgcctccttcatcgaca-3'	5'-gttttgggtccgggttgt-3'	62
Pla2g2d	NM_011109.1	5'-gctctgggctggaactatga-3'	5'-cctgggttgcagttataccg-3'	66
S100a9	NM_009114.2	5'-caccctgagcaagaaggaat-3'	5'-tgtcatttatgaggggcttcattt-3'	31
Rn18s	-	5'-tcgaggccctgtaattggaa-3'	5'-ccctccaatggatcctcgtt-3'	-

Gene	Taq man probe (Applied Biosystems)	Gene	Taq man probe (Applied Biosystems)
Arg1	Mm00475988_m1	Itgam	Mm00434455_m1
Cd68	Mm03047343_m1	Itgax	Mm00498698_m1
Cd206	Mm00485148_m1	Pla2g2d	Mm00478250_m1
Crth2	Mm00438315_s1	Ptgdr	Mm00436050_m1
Ifng	Mm01168134_m1	Ptgds	Mm01330613_m1
Il6	Mm00446190_m1	Ptgds2	Mm00478374_m1
Il10	Mm00439614_m1	Tnf	Mm00443260_g1
Il17a	Mm00439618_m1	Gapdhs	Mouse GAPD (GAPDH), VIC/MGB, 4352339E
Il22	Mm00444241_m1		
Il23a	Mm01160011_g1	Rn18s	Eukatyotic 18S rRNA, VIC/MGB, 4319413E

Confocal Laser Microscopy—Mouse frozen tissues, mounted in OCT compound (Sakura Finetek), were cut into 20-μm-thick sections using a cryomicrotome (CM3050S; Leica). The sections were incubated with 1.5× BlockAce^R (DS Pharma Biomedical) in 10 mM Tris-HCl (pH 7.4) containing 150 mM NaCl (TBS) for 30 min and then with rabbit anti-mouse sPLA₂-IID antibody (59), phycoerythrin-labeled hamster anti-mouse CD11c antibody (N418; eBioscience), or FITC-labeled rat anti-mouse MHC class II (MHC-II) antibody (M5/114.15.2; BioLegend) in TBS containing 0.1% (w/v) bovine serum albumin (TBS/BSA) overnight at 4 °C. The sections were then treated with 1 μg/ml Alexa 647-labeled goat anti-rabbit IgG (Invitrogen) in TBS/BSA for 1 h, mounted in a Vectashield mounting medium (Vector Laboratories), and analyzed with a confocal laser scanning microscope (LSM510 META; Carl Zeiss). The specificity of the anti-sPLA₂-IID antibody was confirmed by absence of sPLA₂-IID staining in the spleen, LNs, and skin of $Pla2g2d^{-/-}$ mice (12).

Flow Cytometry—Flow cytometry was performed as described previously (12, 24). Briefly, mouse inguinal LNs or spleen were excised and minced in Hanks' solution (Nissui Pharmaceutical) with 2% (v/v) heat-inactivated fetal bovine serum (FBS; Invitrogen) and 0.05% (w/v) sodium azide (Nakalai Tesque). Mouse ear skin was incubated with 0.25% (w/v) trypsin-EDTA (Sigma) for 60 min at 37 °C to separate the dermis from the epidermis. These tissues were then incubated with 400 units/ml collagenase type II (Worthington) with shaking for 30 min at 37 °C. After adding 10 mM EDTA, the resulting cell suspensions were passed through a 70-μm

nylon cell strainer (Falcon^TM) and then centrifuged at 300 × *g* for 5 min at 4 °C. The isolated LN cells or splenocytes were treated for 2 min on ice with 10 mM Tris-HCl (pH 7.0) containing 0.84% (w/v) ammonium chloride to lyse red blood cells, centrifuged, and suspended in Hanks' solution. The cells were blocked with mouse BD Tc Block^TM (BD Biosciences), incubated with marker antibodies (listed in Table 2), and analyzed with a FACSAria III (BD Biosciences) and FlowJo (Tree Star) software.

Hapten-induced Contact Dermatitis—On day −5, mice (C57BL/6 background, 8–12-week-old males) were sensitized with 50 μl of 0.5% (w/v) DNFB (Sigma) in acetone/olive oil (4/1; v/v) on the shaved abdominal skin (sensitization phase). On day 0, the dorsal and ventral surfaces of the ears were challenged with 20 μl of 0.3% DNFB (elicitation phase). Ear thickness was monitored with a micrometer. To examine irritant dermatitis (corresponding to the sensitization phase of CHS), the ears were subjected to a single challenge with 50 μl of 0.5% DNFB. At the appropriate time points, the skin and regional LNs from the scarified mice were subjected to quantitative RT-PCR, histochemistry, flow cytometry, and lipidomics analysis, as described previously (12, 24).

IMQ-induced Psoriasis—Mice (C57BL/6 background, 8–12-week-old males) received a daily topical application of 12.5 μg of 5% (w/v) IMQ (Mochida Pharma) on the dorsal and ventral surfaces of the ears over 4 days (total 50 μg of IMQ cream per mouse). Ear thickness was monitored at various time points with a micrometer. On day 6, the skin and LNs from the scarified mice were subjected to quantitative RT-PCR, histochemistry, flow cytometry, and lipidomics analysis, as described previously (24).

Skin Carcinogenesis—The back skin of mice (BALB/c background, 8-week-old female) was shaved with an electric clipper. One week later, 200 μl of 2 mM DMBA (Sigma) in acetone was applied to the shaved skin. After 1 week, 200 μl of 80 μM TPA (Sigma) in acetone was applied to the skin twice a week over 24 weeks. Cutaneous papillomas were counted and scored weekly. At appropriate time points, the skin and LNs from the scarified mice were subjected to quantitative RT-PCR and histochemistry, as described previously (24). Flow cytometry of M1/M2-type macrophages and CD8^+ T cells in the LNs was performed in accordance with the procedure described previously (60).

Cell Culture—Mouse LN cells were cultured in RPMI 1640 medium (Invitrogen) containing 10% heat-inactivated FBS, 2 mM L-glutamine, 25 mM Hepes, 50 μM 2-mercaptoethanol, 1 mM nonessential amino acids, 1 mM sodium pyruvate, 100 units/ml penicillin, and 100 μg/ml streptomycin. Bone marrow cells were cultured with mouse GM-CSF (10 ng/ml; PeproTech) for 9 days and with mouse M-CSF (100 ng/ml; Kyowa Kirin) for 3 days to obtain BMDCs and macrophages, respectively (61). The cells (2 × 10^6 cells/ml) were treated with or without 5 μg/ml IMQ or 100 μg/ml DNBS (Sigma) for appropriate periods. RNA extracted from the cells was taken for quantitative RT-PCR, and the supernatants were subjected to enzyme immunoassay for IFN-γ and IL-17A (eBioscience) or PGD₂ (Cayman Chemicals). As required, the cells were pretreated with 10 nM lipids (Cayman Chemicals) for 30 min and

TABLE 2
A list of antibodies used in flow cytometry
PE indicates phycoerythrin, and APC indicates allophycocyamin.

Molecule	Clone	Subclass	Fluorescent labeling	Source
CD3ϵ	145–2C11	Hamster IgG	FITC	BioLegend
CD4	GK1.5	Rat IgG2b	APC-eFluor 780	eBioscience
CD8α	53-6.7	Rat IgG2a	Pacific Blue	eBioscience
CD11b	M1/70	Rat IgG2b	APC	BioLegend
CD11c	N418	Hamster IgG	PE	eBioscience
CD16/32	93	Rat IgG2a		BioLegend
CD206	C068C2	Rat IgG2a	APC	BioLegend
F4/80	BM8	Rat IgG2a	Pacific Blue	BioLegend
Gr-1	RB6-8C5	Rat IgG2b	APC	BioLegend
			PE	BD Pharmingen
IFN-γ	XMG1.2	Rat IgG1	PE	eBioscience
IL-17A	eBio17B7	Rat IgG2a	APC	eBioscience
IL-22	IL22JOP	Rat IgG2a	APC	eBioscience
MHC-II	M5/114.15.2	Rat IgG2b	FITC	BioLegend
NK1.1	PK136	Mouse IgG2a	APC	eBioscience
TCRβ	H57–597	Hamster IgG	FITC	BioLegend

then stimulated in 200 μl of serum-free X-VIVO medium (Lonza) in the continued presence of the lipids in 96-well U-bottom plates (Iwaki). These procedures were detailed in our previous study (12).

ESI-MS—Samples for ESI-MS of lipids were prepared and analyzed as described previously (12, 24). Briefly, tissues were soaked in 10 volumes of methanol and then homogenized with a Polytron homogenizer. After overnight incubation at −20 °C, water was added to the mixture to give a final methanol concentration of 10% (v/v). As an internal standard, 1 nmol of d_5-labeled EPA and d_4-labeled PGE$_2$ (Cayman Chemicals) was added to each sample. The samples in 10% methanol were applied to Sep-Pak C18 cartridges (Waters), washed with 10 ml of hexane, eluted with 3 ml of methyl formate, dried up under N$_2$ gas, and dissolved in 60% methanol. Analysis of PUFAs and their metabolites was performed using a 4000Q-TRAP quadrupole-linear ion trap hybrid mass spectrometer (AB Sciex) with liquid chromatography (LC-20AP; Shimadzu) combined with an HTC PAL autosampler (CTC Analytics). The samples were applied to a Develosil C30-UG column (1 × 150 mm inner diameter, 3-μm particle) (Nomura Chemical) coupled for ESI-MS/MS. The samples injected by an autosampler (10 μl) were separated using a step gradient with mobile phase C (water containing 0.1% acetic acid) and mobile phase D (acetonitrile/methanol = 4:1; v/v) at a flow rate of 50 μl/min at 45 °C. Identification was conducted using multiple reaction monitoring transition and retention times, and quantification was performed based on the peak area of the multiple reaction monitoring transition and the calibration curve obtained with an authentic standard for each compound (12, 24).

Statistical Analyses—All values are given as the mean ± S.E. Differences between the two groups were assessed by unpaired Student's t test or Mann-Whitney U test using the Excel Statistical Program File ystat 2008 (Igaku Tosho Shuppan, Tokyo, Japan). Differences at p values of less than 0.05 were considered statistically significant.

Author Contributions—Y. M., Y. K., M. S., and K. Y. designed and performed the experiments. Y. T., C. T., and M. H. G. generated mutant mice. K. M. assisted Y. K. and M. S. M. M. wrote the manuscript with input from all the other authors.

References
1. Nathan, C., and Ding, A. (2010) Nonresolving inflammation. *Cell* **140,** 871–882
2. Tabas, I., and Glass, C. K. (2013) Anti-inflammatory therapy in chronic disease: challenges and opportunities. *Science* **339,** 166–172
3. Deutschman, C. S., and Tracey, K. J. (2014) Sepsis: current dogma and new perspectives. *Immunity* **40,** 463–475
4. Hirata, T., and Narumiya, S. (2012) Prostanoids as regulators of innate and adaptive immunity. *Adv. Immunol.* **116,** 143–174
5. Shimizu, T. (2009) Lipid mediators in health and disease: enzymes and receptors as therapeutic targets for the regulation of immunity and inflammation. *Annu. Rev. Pharmacol. Toxicol.* **49,** 123–150
6. Serhan, C. N. (2014) Pro-resolving lipid mediators are leads for resolution physiology. *Nature* **510,** 92–101
7. Serhan, C. N., Chiang, N., and Van Dyke, T. E. (2008) Resolving inflammation: dual anti-inflammatory and pro-resolution lipid mediators. *Nat. Rev. Immunol.* **8,** 349–361
8. Dalli, J., Chiang, N., and Serhan, C. N. (2015) Elucidation of novel 13-series resolvins that increase with atorvastatin and clear infections. *Nat. Med.* **21,** 1071–1075
9. Chiang, N., Dalli, J., Colas, R. A., and Serhan, C. N. (2015) Identification of resolvin D2 receptor mediating resolution of infections and organ protection. *J. Exp. Med.* **212,** 1203–1217
10. Arita, M., Bianchini, F., Aliberti, J., Sher, A., Chiang, N., Hong, S., Yang, R., Petasis, N. A., and Serhan, C. N. (2005) Stereochemical assignment, anti-inflammatory properties, and receptor for the ω-3 lipid mediator resolvin E1. *J. Exp. Med.* **201,** 713–722
11. Endo, J., Sano, M., Isobe, Y., Fukuda, K., Kang, J. X., Arai, H., and Arita, M. (2014) 18-HEPE, an n-3 fatty acid metabolite released by macrophages, prevents pressure overload-induced maladaptive cardiac remodeling. *J. Exp. Med.* **211,** 1673–1687
12. Miki, Y., Yamamoto, K., Taketomi, Y., Sato, H., Shimo, K., Kobayashi, T., Ishikawa, Y., Ishii, T., Nakanishi, H., Ikeda, K., Taguchi, R., Kabashima, K., Arita, M., Arai, H., Lambeau, G., *et al.* (2013) Lymphoid tissue phospholipase A$_2$ group IID resolves contact hypersensitivity by driving antiinflammatory lipid mediators. *J. Exp. Med.* **210,** 1217–1234
13. Sawada, Y., Honda, T., Hanakawa, S., Nakamizo, S., Murata, T., Ueharaguchi-Tanada, Y., Ono, S., Amano, W., Nakajima, S., Egawa, G., Tanizaki, H., Otsuka, A., Kitoh, A., Dainichi, T., Ogawa, N., *et al.* (2015) Resolvin E1 inhibits dendritic cell migration in the skin and attenuates contact hypersensitivity responses. *J. Exp. Med.* **212,** 1921–1930
14. Murase, R., Sato, H., Yamamoto, K., Ushida, A., Nishito, Y., Ikeda, K.,

Kobayashi, T., Yamamoto, T., Taketomi, Y., and Murakami, M. (2016) Group X secreted phospholipase A$_2$ releases ω3 polyunsaturated fatty acids, suppresses colitis, and promotes sperm fertility. *J. Biol. Chem.* **291,** 6895–6911

15. Uozumi, N., Kume, K., Nagase, T., Nakatani, N., Ishii, S., Tashiro, F., Komagata, Y., Maki, K., Ikuta, K., Ouchi, Y., Miyazaki, J., and Shimizu, T. (1997) Role of cytosolic phospholipase A$_2$ in allergic response and parturition. *Nature* **390,** 618–622

16. Leslie, C. C. (2015) Cytosolic phospholipase A$_2$: physiological function and role in disease. *J. Lipid Res.* **56,** 1386–1402

17. Ueno, N., Taketomi, Y., Yamamoto, K., Hirabayashi, T., Kamei, D., Kita, Y., Shimizu, T., Shinzawa, K., Tsujimoto, Y., Ikeda, K., Taguchi, R., and Murakami, M. (2011) Analysis of two major intracellular phospholipases A$_2$ (PLA$_2$) in mast cells reveals crucial contribution of cytosolic PLA$_2$α, not Ca^{2+}-independent PLA$_2$β, to lipid mobilization in proximal mast cells and distal fibroblasts. *J. Biol. Chem.* **286,** 37249–37263

18. Murakami, M., Sato, H., Miki, Y., Yamamoto, K., and Taketomi, Y. (2015) A new era of secreted phospholipase A$_2$. *J. Lipid Res.* **56,** 1248–1261

19. Murakami, M., Taketomi, Y., Miki, Y., Sato, H., Hirabayashi, T., and Yamamoto, K. (2011) Recent progress in phospholipase A$_2$ research: from cells to animals to humans. *Prog Lipid Res* **50,** 152–192

20. Lambeau, G., and Gelb, M. H. (2008) Biochemistry and physiology of mammalian secreted phospholipases A$_2$. *Annu. Rev. Biochem.* **77,** 495–520

21. Taketomi, Y., Ueno, N., Kojima, T., Sato, H., Murase, R., Yamamoto, K., Tanaka, S., Sakanaka, M., Nakamura, M., Nishito, Y., Kawana, M., Kambe, N., Ikeda, K., Taguchi, R., Nakamizo, S., *et al.* (2013) Mast cell maturation is driven via a group III phospholipase A$_2$-prostaglandin D$_2$-DP1 receptor paracrine axis. *Nat. Immunol.* **14,** 554–563

22. Sato, H., Taketomi, Y., Isogai, Y., Miki, Y., Yamamoto, K., Masuda, S., Hosono, T., Arata, S., Ishikawa, Y., Ishii, T., Kobayashi, T., Nakanishi, H., Ikeda, K., Taguchi, R., Hara, S., *et al.* (2010) Group III secreted phospholipase A$_2$ regulates epididymal sperm maturation and fertility in mice. *J. Clin. Invest.* **120,** 1400–1414

23. Sato, H., Taketomi, Y., Ushida, A., Isogai, Y., Kojima, T., Hirabayashi, T., Miki, Y., Yamamoto, K., Nishito, Y., Kobayashi, T., Ikeda, K., Taguchi, R., Hara, S., Ida, S., Miyamoto, Y., *et al.* (2014) The adipocyte-inducible secreted phospholipases PLA2G5 and PLA2G2E play distinct roles in obesity. *Cell Metab.* **20,** 119–132

24. Yamamoto, K., Miki, Y., Sato, M., Taketomi, Y., Nishito, Y., Taya, C., Muramatsu, K., Ikeda, K., Nakanishi, H., Taguchi, R., Kambe, N., Kabashima, K., Lambeau, G., Gelb, M. H., and Murakami, M. (2015) The role of group IIF-secreted phospholipase A$_2$ in epidermal homeostasis and hyperplasia. *J. Exp. Med.* **212,** 1901–1919

25. Henderson, W. R., Jr., Chi, E. Y., Bollinger, J. G., Tien, Y. T., Ye, X., Castelli, L., Rubtsov, Y. P., Singer, A. G., Chiang, G. K., Nevalainen, T., Rudensky, A. Y., and Gelb, M. H. (2007) Importance of group X-secreted phospholipase A$_2$ in allergen-induced airway inflammation and remodeling in a mouse asthma model. *J. Exp. Med.* **204,** 865–877

26. Boilard, E., Lai, Y., Larabee, K., Balestrieri, B., Ghomashchi, F., Fujioka, D., Gobezie, R., Coblyn, J. S., Weinblatt, M. E., Massarotti, E. M., Thornhill, T. S., Divangahi, M., Remold, H., Lambeau, G., Gelb, M. H., *et al.* (2010) A novel anti-inflammatory role for secretory phospholipase A$_2$ in immune complex-mediated arthritis. *EMBO Mol. Med.* **2,** 172–187

27. Ohta, S., Imamura, M., Xing, W., Boyce, J. A., and Balestrieri, B. (2013) Group V secretory phospholipase A$_2$ is involved in macrophage activation and is sufficient for macrophage effector functions in allergic pulmonary inflammation. *J. Immunol.* **190,** 5927–5938

28. Vijay, R., Hua, X., Meyerholz, D. K., Miki, Y., Yamamoto, K., Gelb, M., Murakami, M., and Perlman, S. (2015) Critical role of phospholipase A$_2$ group IID in age-related susceptibility to severe acute respiratory syndrome-CoV infection. *J. Exp. Med.* **212,** 1851–1868

29. von Allmen, C. E., Schmitz, N., Bauer, M., Hinton, H. J., Kurrer, M. O., Buser, R. B., Gwerder, M., Muntwiler, S., Sparwasser, T., Beerli, R. R., and Bachmann, M. F. (2009) Secretory phospholipase A$_2$-IID is an effector molecule of CD4$^+$CD25$^+$ regulatory T cells. *Proc. Natl. Acad. Sci. U.S.A.* **106,** 11673–11678

30. Yamamoto, Y., Otani, S., Hirai, H., Nagata, K., Aritake, K., Urade, Y., Narumiya, S., Yokozeki, H., Nakamura, M., and Satoh, T. (2011) Dual functions of prostaglandin D$_2$ in murine contact hypersensitivity via DP and CRTH2. *Am. J. Pathol.* **179,** 302–314

31. Takeshita, K., Yamasaki, T., Nagao, K., Sugimoto, H., Shichijo, M., Gantner, F., and Bacon, K. B. (2004) CRTH2 is a prominent effector in contact hypersensitivity-induced neutrophil inflammation. *Int. Immunol.* **16,** 947–959

32. Hammad, H., Kool, M., Soullié, T., Narumiya, S., Trottein, F., Hoogsteden, H. C., and Lambrecht, B. N. (2007) Activation of the D prostanoid 1 receptor suppresses asthma by modulation of lung dendritic cell function and induction of regulatory T cells. *J. Exp. Med.* **204,** 357–367

33. Tortola, L., Rosenwald, E., Abel, B., Blumberg, H., Schäfer, M., Coyle, A. J., Renauld, J. C., Werner, S., Kisielow, J., and Kopf, M. (2012) Psoriasiform dermatitis is driven by IL-36-mediated DC-keratinocyte crosstalk. *J. Clin. Invest.* **122,** 3965–3976

34. Condeelis, J., and Pollard, J. W. (2006) Macrophages: obligate partners for tumor cell migration, invasion, and metastasis. *Cell* **124,** 263–266

35. Serhan, C. N. (2007) Resolution phase of inflammation: novel endogenous anti-inflammatory and proresolving lipid mediators and pathways. *Annu. Rev. Immunol.* **25,** 101–137

36. Dalli, J., Zhu, M., Vlasenko, N. A., Deng, B., Haeggström, J. Z., Petasis, N. A., and Serhan, C. N. (2013) The novel 13S,14S-epoxy-maresin is converted by human macrophages to maresin 1 (MaR1), inhibits leukotriene A$_4$ hydrolase (LTA$_4$H), and shifts macrophage phenotype. *FASEB J.* **27,** 2573–2583

37. Titos, E., Rius, B., González-Périz, A., López-Vicario, C., Morán-Salvador, E., Martínez-Clemente, M., Arroyo, V., and Clària, J. (2011) Resolvin D1 and its precursor docosahexaenoic acid promote resolution of adipose tissue inflammation by eliciting macrophage polarization toward an M2-like phenotype. *J. Immunol.* **187,** 5408–5418

38. Schwab, J. M., Chiang, N., Arita, M., and Serhan, C. N. (2007) Resolvin E1 and protectin D1 activate inflammation-resolution programmes. *Nature* **447,** 869–874

39. Spite, M., Norling, L. V., Summers, L., Yang, R., Cooper, D., Petasis, N. A., Flower, R. J., Perretti, M., and Serhan, C. N. (2009) Resolvin D2 is a potent regulator of leukocytes and controls microbial sepsis. *Nature* **461,** 1287–1291

40. Chiang, N., Fredman, G., Bäckhed, F., Oh, S. F., Vickery, T., Schmidt, B. A., and Serhan, C. N. (2012) Infection regulates pro-resolving mediators that lower antibiotic requirements. *Nature* **484,** 524–528

41. Jia, Q., Lupton, J. R., Smith, R., Weeks, B. R., Callaway, E., Davidson, L. A., Kim, W., Fan, Y. Y., Yang, P., Newman, R. A., Kang, J. X., McMurray, D. N., and Chapkin, R. S. (2008) Reduced colitis-associated colon cancer in Fat-1 (n-3 fatty acid desaturase) transgenic mice. *Cancer Res.* **68,** 3985–3991

42. Kim, W., Khan, N. A., McMurray, D. N., Prior, I. A., Wang, N., and Chapkin, R. S. (2010) Regulatory activity of polyunsaturated fatty acids in T-cell signaling. *Prog. Lipid Res.* **49,** 250–261

43. Ramon, S., Gao, F., Serhan, C. N., and Phipps, R. P. (2012) Specialized proresolving mediators enhance human B cell differentiation to antibody-secreting cells. *J. Immunol.* **189,** 1036–1042

44. Krishnamoorthy, S., Recchiuti, A., Chiang, N., Yacoubian, S., Lee, C. H., Yang, R., Petasis, N. A., and Serhan, C. N. (2010) Resolvin D1 binds human phagocytes with evidence for proresolving receptors. *Proc. Natl. Acad. Sci. U.S.A.* **107,** 1660–1665

45. Diep, Q. N., Touyz, R. M., and Schiffrin, E. L. (2000) PPARα activator effects on Ang II-induced vascular oxidative stress and inflammation. *Hypertension* **36,** 851–855

46. Ariyama, H., Kono, N., Matsuda, S., Inoue, T., and Arai, H. (2010) Decrease in membrane phospholipid unsaturation induces unfolded protein response. *J. Biol. Chem.* **285,** 22027–22035

47. Holzer, R. G., Park, E. J., Li, N., Tran, H., Chen, M., Choi, C., Solinas, G., and Karin, M. (2011) Saturated fatty acids induce c-Src clustering within membrane subdomains, leading to JNK activation. *Cell* **147,** 173–184

48. Oh, D. Y., Talukdar, S., Bae, E. J., Imamura, T., Morinaga, H., Fan, W., Li, P., Lu, W. J., Watkins, S. M., and Olefsky, J. M. (2010) GPR120 is an ω-3 fatty acid receptor mediating potent anti-inflammatory and insulin-sensitizing effects. *Cell* **142,** 687–698

49. Ichimura, A., Hirasawa, A., Poulain-Godefroy, O., Bonnefond, A., Hara,

T., Yengo, L., Kimura, I., Leloire, A., Liu, N., Iida, K., Choquet, H., Besnard, P., Lecoeur, C., Vivequin, S., Ayukawa, K., *et al.* (2012) Dysfunction of lipid sensor GPR120 leads to obesity in both mouse and human. *Nature* **483,** 350–354

50. Yan, Y., Jiang, W., Spinetti, T., Tardivel, A., Castillo, R., Bourquin, C., Guarda, G., Tian, Z., Tschopp, J., and Zhou, R. (2013) ω-3 fatty acids prevent inflammation and metabolic disorder through inhibition of NLRP3 inflammasome activation. *Immunity* **38,** 1154–1163

51. Makide, K., Uwamizu, A., Shinjo, Y., Ishiguro, J., Okutani, M., Inoue, A., and Aoki, J. (2014) Novel lysophosphoplipid receptors: their structure and function. *J. Lipid Res.* **55,** 1986–1995

52. Barnes, M. J., Li, C. M., Xu, Y., An, J., Huang, Y., and Cyster, J. G. (2015) The lysophosphatidylserine receptor GPR174 constrains regulatory T cell development and function. *J. Exp. Med.* **212,** 1011–1020

53. Boudreau, L. H., Duchez, A. C., Cloutier, N., Soulet, D., Martin, N., Bollinger, J., Paré, A., Rousseau, M., Naika, G. S., Lévesque, T., Laflamme, C., Marcoux, G., Lambeau, G., Farndale, R. W., Pouliot, M., *et al.* (2014) Platelets release mitochondria serving as substrate for bactericidal group IIA-secreted phospholipase A₂ to promote inflammation. *Blood* **124,** 2173–2183

54. Pernet, E., Guillemot, L., Burgel, P. R., Martin, C., Lambeau, G., Sermet-Gaudelus, I., Sands, D., Leduc, D., Morand, P. C., Jeammet, L., Chignard, M., Wu, Y., and Touqui, L. (2014) *Pseudomonas aeruginosa* eradicates *Staphylococcus aureus* by manipulating the host immunity. *Nat. Commun.* **5,** 5105

55. Rubio, J. M., Rodríguez, J. P., Gil-de-Gómez, L., Guijas, C., Balboa, M. A., and Balsinde, J. (2015) Group V secreted phospholipase A₂ is upregulated by IL-4 in human macrophages and mediates phagocytosis via hydrolysis of ethanolamine phospholipids. *J. Immunol.* **194,** 3327–3339

56. Balestrieri, B., Maekawa, A., Xing, W., Gelb, M. H., Katz, H. R., and Arm, J. P. (2009) Group V secretory phospholipase A₂ modulates phagosome maturation and regulates the innate immune response against *Candida albicans*. *J. Immunol.* **182,** 4891–4898

57. Ohtsuki M, Taketomi Y, Arata S, Masuda S, Ishikawa Y, Ishii T, Takanezawa Y, Aoki J, Arai H, Yamamoto K, Kudo I, Murakami M. (2006) Transgenic expression of group V, but not group X, secreted phospholipase A₂ in mice leads to neonatal lethality because of lung dysfunction. *J. Biol. Chem.* **281,** 36420–36433

58. Kanegae, Y., Takamori, K., Sato, Y., Lee, G., Nakai, M., and Saito, I. (1996) Efficient gene activation system on mammalian cell chromosomes using recombinant adenovirus producing Cre recombinase. *Gene* **181,** 207–212

59. Degousee, N., Ghomashchi, F., Stefanski, E., Singer, A., Smart, B. P., Borregaard, N., Reithmeier, R., Lindsay, T. F., Lichtenberger, C., Reinisch, W., Lambeau, G., Arm, J., Tischfield, J., Gelb, M. H., and Rubin, B. B. (2002) Groups IV, V, and X phospholipases A₂s in human neutrophils: role in eicosanoid production and gram-negative bacterial phospholipid hydrolysis. *J. Biol. Chem.* **277,** 5061–5073

60. Ohtsuki, T., Kimura, K., Tokunaga, Y., Tsukiyama-Kohara, K., Tateno, C., Hayashi, Y., Hishima, T., and Kohara, M. (2016) M2 macrophages play critical roles in progression of inflammatory liver disease in hepatitis C virus transgenic mice. *J. Virol.* **90,** 300–307

61. Lutz, M. B., Kukutsch, N., Ogilvie, A. L., Rössner, S., Koch, F., Romani, N., and Schuler, G. (1999) An advanced culture method for generating large quantities of highly pure dendritic cells from mouse bone marrow. *J. Immunol. Methods* **223,** 77–92